Motion control for UAV-UGV cooperation with visibility constraint

Conference Paper · September 2015

DOI: 10.1109/CCA.2015.7320804

3 authors, including:

Saman Khodaverdian
Technische Universität Darmstadt
21 PUBLICATIONS **43** CITATIONS
SEE PROFILE

Volker Willert
Hochschule für angewandte Wissenschaften Würzburg-Schweinfurt
111 PUBLICATIONS **901** CITATIONS
SEE PROFILE

Motion Control for UAV-UGV Cooperation with Visibility Constraint

Lukas Klodt, Saman Khodaverdian and Volker Willert

***Abstract*— The subject of this paper is a cooperative scenario where an unmanned aerial vehicle (UAV) assists an unmanned ground vehicle (UGV) to achieve a higher level task. We assume that the UAV detects the UGV within a certain range with a vision sensor. While satisfying this constraint, the UAV can provide relative information about any events of interest in its field of view. The focus is on the motion control of the UAV relative to the UGV. To this end, we present a new control law that combines an extended dynamic coverage strategy with a tracking controller. Different weighting functions to combine the controllers are evaluated. The results are further compared with a second motion strategy introduced for this purpose. Both control laws guarantee that the UAV will maintain visual contact while making use of available mobility as much as possible, allowing the UAV to gather more information and act as an anticipatory element.**

I. INTRODUCTION

There is an increasing amount of possibilities for meaningful use of cooperative multi-robot systems in many different situations. A prominent application example is the use of mobile robots in search and rescue scenarios or emergency response situations. Advances in technology make the deployments more valuable from day to day. However, an important aspect in such situations is that the robot systems have a certain degree of autonomy, especially when multiple possibly heterogeneous vehicles interact or cooperate. Our goal is to relieve operators from difficult control tasks and make systems more independent when the communication is restricted.

Recently, cooperative control tasks for networked systems have been considered in different research areas. Often, it is desired to have some kind of collective behavior, as for instance swarming or flocking ([1], [2]), or a special formation ([3]), possibly with obstacle avoidance ([4]). Usually, for the aforementioned tasks it is desired that the robots or agents achieve some special formation with a certain distance between the agents. This results in a synchronous behavior where all agents act equally to satisfy the overall goal. A popular method in this area is the use of potential forces, as in [5], where a group of fixed wing UAVs circles the centroid of a ground vehicle formation.

The specific setting under consideration here is a cooperative UAV-UGV mission, where the motion of the ground vehicle is controlled independently (either by performing a task autonomously or via teleoperation) and a priori unknown. The aerial vehicle is meant to assist the ground vehicle by acting like an extended (mobile) sensor device that provides additional information through complementary sensors onboard the UAV and the different field of view. The UAV can provide information that might not be available to the UGV at all (e.g. detecting negative obstacles, surface irregularities, type of terrain etc.) or provides information earlier than the UGV would be able to detect with its own sensors. Similar types of systems have been introduced in [6], [7], [8], [9].

For this to be possible, relative localization between the vehicles is required. Since GPS is only available in outdoor scenarios (cf. [10], [11]) and point cloud alignment [12] requires an overlap between the sensor data, we will focus on relative localization through direct visibility.

Visibility-based relative localization can be realized in different ways, e.g. by detecting the UAV hovering above the UGV with a camera mounted on the ground robot. Cooperative scenarios with this approach have been proposed in [13], [14]. The reverse detection direction is also possible, as demonstrated in [15] among others. In [16], a visibility-constrained formation approach for a group of ground and aerial vehicles is introduced and solved with a model-predictive control approach. A different vision-based approach is described in [17], where the UAV maps an area of interest based on given waypoints and then guides a UGV through obstacles with the gathered camera data.

In contrast to existing approaches, we deliberately use the region of visibility and the higher mobility of the UAV to gather additional information. To the best of our knowledge, this idea has not been investigated specifically for UAV-UGV systems. We propose and compare two different control laws for motion of the UAV: 1) An extension of a dynamic coverage approach presented in [18], [19] to double integrator systems with a time-varying region of interest. 2) A virtual point tracking method, demonstrated with a circular motion around the ground vehicle's position. For both cases, we can guarantee that the visibility constraint is satisfied at all times. To this end, we use a tracking controller that is easily parametrized with well-known methods from control theory. The new combined control law is presented in a general form and different weighting functions to combine the tracking with the coverage strategy are evaluated.

II. PROBLEM FORMULATION

We consider two types of vehicles, namely UGVs and UAVs. Variables associated with a specific type of vehicle will be denoted with the indices g and a for ground or aerial respectively. Even though the UAV moves in 3-dimensional space, the flight altitude can be considered decoupled from the planar position given our assumptions. Specifying a

This work was supported by the German Research Foundation (DFG) within the GRK 1362.

All authors are with the Institute of Automatic Control and Mechatronics, Technische Universität Darmstadt, Germany
{lklodt, khodaver, vwillert}@rmr.tu-darmstadt.de

constant altitude, both vehicles will be moving in a convex and bounded environment $\mathcal{Q} \subset \mathbb{R}^2$ on different height levels. Omnidirectional ground vehicles as well as rotorcraft aerial vehicles during low velocity and acceleration flight can both be modeled by double integrator dynamics

$$\ddot{\boldsymbol{p}}(t) = \boldsymbol{u}(t), \quad \|\boldsymbol{u}(t)\| \leq u_{max}, \quad \|\dot{\boldsymbol{p}}(t)\| \leq v_{max} \tag{1}$$

with $\boldsymbol{p}, \boldsymbol{u} \in \mathbb{R}^2$ denoting robot position and control input and $u_{max}, v_{max} \in \mathbb{R}_+$ denoting input and velocity constraints. To allow for higher mobility of the UAV compared to the UGV we always assume $v_{a,max} > v_{g,max}$ and $u_{a,max} > u_{g,max}$. If the context is clear, time dependencies of most variables will be omitted hereafter.

Moving to a target location $\overline{\boldsymbol{p}} \in \mathcal{Q}$ with the UGV can be realized by a stabilizing controller $\boldsymbol{u}_g = \boldsymbol{f}(\boldsymbol{p}_g, \overline{\boldsymbol{p}})$. The goal location $\overline{\boldsymbol{p}}$ is constant until $\|\boldsymbol{p}_g - \overline{\boldsymbol{p}}\| < \epsilon$, for a small $\epsilon > 0$, and then the next goal location is approached. Therefore, the trajectory of the UGV consists of straight line segments.

The sensor model of the UAV is defined by a hill-shaped coverage function $S_a : \mathcal{Q} \times \mathbb{R}^2 \to \mathbb{R}_+$ for vision-based aerial mapping as proposed in [19]:

$$S_a(\boldsymbol{p}_a, \boldsymbol{q}) = \begin{cases} \frac{M_a}{r^4}(\|\boldsymbol{p}_a - \boldsymbol{q}\|^2 - r^2)^2, & \text{if } \|\boldsymbol{p}_a - \boldsymbol{q}\| \leq r \\ 0, & \text{if } \|\boldsymbol{p}_a - \boldsymbol{q}\| > r. \end{cases} \tag{2}$$

This function describes how effective the UAV senses a point $\boldsymbol{q} \in \mathcal{Q}$ given its current position, where the sensing quality will be highest at $\boldsymbol{q} = \boldsymbol{p}_a$ with a peak value of M_a and zero outside of the sensory range r. Note that (2) is only an example of a possible sensor formulation that could be replaced by any other differentiable function that models the characteristics of a given sensor.

The effective coverage accumulated at a point $\boldsymbol{q}$ can now be defined by

$$C(\boldsymbol{q}, t) := \int_0^t S_a(\boldsymbol{p}_a(\tau), \boldsymbol{q}) d\tau \tag{3}$$

and can be interpreted as confidence level about the information attained at that point until time t. To evaluate the current coverage with respect to a *desired coverage* C^* the following error function is used:

$$e(t) = \int_{\mathcal{Q}} h(C^* - C(\boldsymbol{q}, t)) \phi(\boldsymbol{q}, \boldsymbol{p}_g) d\boldsymbol{q}. \tag{4}$$

The scalar function $h(x)$ penalizes lack of coverage and can be set to $h(x) = (\max(0, x))^2$ to satisfy certain conditions according to [19]. An additional weighting is achieved by using a *density* function $\phi : \mathcal{Q} \times \mathbb{R}^2 \to \mathbb{R}_{\geq 0}$ that will be specified more precisely in Section III. As long as the coverage at any point in $\mathcal{Q}$ is below C^* the error will be positive. Otherwise, if $C(\boldsymbol{q}, t) \geq C^*$ for all $\boldsymbol{q} \in \mathcal{Q}$, $e(t)$ will be zero since higher coverage values are not penalized.

Finally, the visibility constraint to guarantee relative localization is given by

$$\|\boldsymbol{p}_a - \boldsymbol{p}_g\| < r_v \tag{5}$$

with $r_v \in \mathbb{R}_+$, $r_v < r$ such that the UGV can always be reliably detected by the UAV.

With these preliminaries, the problem statement can be formulated: Find a stabilizing control law $\boldsymbol{u}_a$ for the UAV with dynamics as in (1) that minimizes (4) while maintaining the constraint in (5) for all t.

III. DYNAMIC COVERAGE

In the upcoming section a control law for dynamic coverage is revisited and our adaptations and extensions for the current problem are explained.

A. Original Approach

In [19], a local gradient-type control law for single integrator vehicles $\dot{\boldsymbol{p}} = \boldsymbol{u}_{si}$ is proposed, given by

$$\boldsymbol{u}_{cov} = k \frac{4M}{r^4} \int_{\mathcal{Q}_r} h'(C^* - C(\boldsymbol{q}, t)) \cdot (\|\boldsymbol{p}_a - \boldsymbol{q}\|^2 - r^2)(\boldsymbol{p}_a - \boldsymbol{q}) \phi(\boldsymbol{q}, \boldsymbol{p}_g) d\boldsymbol{q} \tag{6}$$

with $\mathcal{Q}_r = \{\boldsymbol{q} \in \mathcal{Q} | \|\boldsymbol{p}_a - \boldsymbol{q}\| \leq r\}$, $h'(x) = \frac{\mathrm{d}h(x)}{\mathrm{d}x}$ and $k > 0$. For $\boldsymbol{u}_{si} = \boldsymbol{u}_{cov}$, the single integrator will converge to a state where $\boldsymbol{u}_{cov} = \boldsymbol{0}$ but it is not guaranteed that the error will be zero, due to symmetry or cases where the sensory domain $\mathcal{Q}_r$ is completely covered (i.e. $C(\boldsymbol{q}, t) \geq C^*$ for all $\boldsymbol{q} \in \mathcal{Q}_r$).

To this end, a second control law is introduced. Define a point $\tilde{\boldsymbol{q}}$ that satisfies the following three conditions:

1) $\tilde{\boldsymbol{q}} \in \mathcal{Q}_e$ with $\mathcal{Q}_e = \{\boldsymbol{q} \in \mathcal{Q} | C(\boldsymbol{q}, t) < C^*\}$
2) $\phi(\tilde{\boldsymbol{q}}, \boldsymbol{p}_g) \neq 0$
3) $\tilde{\boldsymbol{q}} = \text{argmin}_{\tilde{\boldsymbol{q}} \in \mathcal{Q}_e} \|\boldsymbol{p}_a - \tilde{\boldsymbol{q}}\|$

Approaching $\tilde{\boldsymbol{q}}$ (which is fixed for some time interval) can be realized with a simple linear feedback controller

$$\tilde{\boldsymbol{u}}_{cov} = k(\tilde{\boldsymbol{q}} - \boldsymbol{p}_a). \tag{7}$$

If there are multiple points that fulfill all three criteria one can be picked randomly. We can now restate a variant of Theorem III.1 from [18], [19].

Lemma 1: Assuming $\phi(\boldsymbol{q}, \boldsymbol{p}_g)$ is static, a single integrator agent with $\dot{\boldsymbol{p}} = \boldsymbol{u}_{si}$ and a sensor model similar to (2) and (3) using the control law

$$\boldsymbol{u}_{si} = \begin{cases} \boldsymbol{u}_{cov}, & \text{if } \boldsymbol{u}_{cov} \neq 0 \\ \tilde{\boldsymbol{u}}_{cov}, & \text{if } \boldsymbol{u}_{cov} = 0 \end{cases} \tag{8}$$

drives the error $e(t) \to 0$ as $t \to \infty$.

A proof and stability discussion for this switching control strategy can be found in the references above.

B. Extensions

The first adaptation that we make is motivated by our visibility constraint. The maximum region the UAV can cover while still respecting (5) is a circle with radius $r_o = r_v + r$ centered at $\boldsymbol{p}_g$. Giving higher priority to points closer to the UGV, we define

$$\phi(\boldsymbol{q}, \boldsymbol{p}_g) = \begin{cases} \cos(\frac{\|\boldsymbol{p}_g - \boldsymbol{q}\|}{r_o}\pi) + 1, & \text{if } \|\boldsymbol{p}_g - \boldsymbol{q}\| \leq r_o \\ 0, & \text{if } \|\boldsymbol{p}_g - \boldsymbol{q}\| > r_o. \end{cases} \tag{9}$$

As opposed to [19], this definition provides a time-varying density that characterizes the region of importance and limits the area to cover relative to the UGV position. The idea of

a time-varying density function has also been considered in an adversarial multi-agent scenario in [20].

The second adaptation becomes necessary due to the vehicle dynamics (1). We will first consider the unconstrained system (i.e. $v_{a,max}$ and $u_{a,max}$ are infinite) and then discuss the case of limited input and velocity. Because (6) is a gradient-type control law it specifies a direction where the error is high and can be reduced by moving in this direction. In a single integrator system, the velocity while following (8) will always be $\dot{\boldsymbol{p}} = \boldsymbol{u}_{si}$, i.e. $\boldsymbol{u}_{si}$ can be seen as a desired velocity vector. By specifying a nominal value for the magnitude of the velocity $v_{ref} \in \mathbb{R}_+$, consider the following control error:

$$\boldsymbol{e}_{vel} = \begin{cases} \frac{\boldsymbol{u}_{si}}{\|\boldsymbol{u}_{si}\|} v_{ref} - \dot{\boldsymbol{p}}_a, & \text{if } e(t) \neq 0 \\ -\dot{\boldsymbol{p}}_a, & \text{if } e(t) = 0. \end{cases} \tag{10}$$

The normalization of the desired velocity provides the advantage that the gain k in (6) and (7) does not have to be determined and the vehicle moves at a higher velocity even when $\boldsymbol{u}_{cov}$ is very small (a problem that we encountered during simulations). In cases where the error becomes zero, a direction of motion is not defined and the vehicle simply decelerates.

From (9), it is obvious that $e(t)$ can never converge to zero permanently as long as the UGV is moving into uncovered regions.

Proposition 1: If $\dot{\boldsymbol{p}}_g(t) = \boldsymbol{0}$ for all $t > t_s$ and any $t_s \geq 0$, a vehicle with dynamics as in (1) and a sensor model given by (2) and (3) using the control law

$$\boldsymbol{u}_{a,cov} = k_v \boldsymbol{e}_{vel}, \tag{11}$$

with $\boldsymbol{e}_{vel}$ from (10), drives $e(t) \to 0$ as $t \to \infty$ for any $k_v > 0$.

Proof: As long as the set $\mathcal{Q}_r^* = \{\boldsymbol{q} \in \mathcal{Q}_r | C(\boldsymbol{q}, t) < C^*, \phi(\boldsymbol{q}, \boldsymbol{p}_g) \neq 0\}$ is nonempty, one has $\boldsymbol{u}_{cov} \neq \boldsymbol{0}$ and $\dot{e}(t) < 0$, i.e. the error decreases. If for any reason $\mathcal{Q}_r^* = \emptyset$, one has $\dot{e}(t) = 0$, switching occurs to $\boldsymbol{u}_{si} = \tilde{\boldsymbol{u}}_{cov}$. In this case, inserting (10), (8) and (7) into (11) yields

$$\boldsymbol{u}_{a,cov} = \frac{k_v v_{ref}}{\|\tilde{\boldsymbol{q}} - \boldsymbol{p}_a\|} (\tilde{\boldsymbol{q}} - \boldsymbol{p}_a) - k_v \dot{\boldsymbol{p}}_a. \tag{12}$$

Without loss of generality, $\tilde{\boldsymbol{q}}$ can be considered a constant reference input and (12) provides an asymptotically stable system for any initial state and $k_v, v_{ref} > 0$. This can be shown by formulating the position error $\boldsymbol{e}_p = \tilde{\boldsymbol{q}} - \boldsymbol{p}_a$ and deriving the error dynamics $\ddot{\boldsymbol{e}}_{\boldsymbol{p}} + k_v \dot{\boldsymbol{e}}_{\boldsymbol{p}} + \frac{k_v v_{ref}}{\|\tilde{\boldsymbol{q}} - \boldsymbol{p}_a\|} \boldsymbol{e}_p = 0$. The equation describes a stable system for any point in time due to the positive coefficients. Hence, the vehicle position $\boldsymbol{p}_a$ approaches $\tilde{\boldsymbol{q}}$ and will be inside a ball of radius $\epsilon_q < r$ around $\tilde{\boldsymbol{q}}$ at some time $\tilde{t}$. At this point $\mathcal{Q}_r^*$ is nonempty again, $\boldsymbol{u}_{si} = \boldsymbol{u}_{cov}$ and $\dot{e}(t) < 0$ for some time interval. This process repeats until $e(t) = 0$ and convergence is guaranteed since $\mathcal{Q}$ is bounded. ∎

Note that Proposition 1 is also valid for the constrained system with $v_{a,max}, u_{a,max} < \infty$. The maximum velocity can be ignored by choosing $v_{ref} \leq v_{a,max}$. The main difference is caused by the limited control input: In case of unlimited $\boldsymbol{u}_a$ the velocity controller can track the desired velocity with arbitrarily high accuracy by using a high value for k_v. Otherwise the error norm $\|\boldsymbol{e}_{vel}\|$ may be high, depending on the quotient $\frac{v_{ref}}{u_{a,max}}$, which can cause the vehicle to leave the area $\mathcal{Q}$. A safety distance to the boundary becomes necessary depending on the choice of the parameters. This safety distance can be calculated just as the result presented in Proposition 2 later in Section V-A.

C. Simulation Example

To get a first impression of the coverage behavior, Fig. 1 shows an example where the UGV is moving along a straight line and the UAV applies the control law given in (11). Systems parameters and further details are described in Section VI.

The velocity error for two different values of k_v is obviously much lower for higher k_v and only has a few remaining peaks if the gain is high enough. This supports the assumption that $\boldsymbol{u}_{cov}$ changes slowly and is consistent most of the time w.r.t. the position of the vehicle (a slight change in position will change $\boldsymbol{u}_{cov}$ only slightly). The peaks in Fig. 1(b) correspond to situations where the direction of $\boldsymbol{u}_{si}$ changes significantly, most often when switching to the symmetry breaking controller (7).

Fig. 1(c) shows how the error $e(t)$ converges to zero for different k_v and also for the constrained system ($k_v = 10.0$ (con.)), i.e. with limited input and velocity. Note that the error can increase as long as the UGV is moving because of the definition of $\phi(\boldsymbol{q}, \boldsymbol{p}_g)$.

As one can see in Fig. 1(a) the UAV has left the circle with radius r_v around $\boldsymbol{p}_g$. Therefore, we need an additional motion component that guarantees that the visibility condition is satisfied.

IV. TRACKING CONTROL

In the following, we present a tracking control strategy for the UAV. Note that the visibility boundary (5) not only depends on the motion of the UAV, but also on the motion of the UGV. Thus, the UAV needs to follow the UGV to ensure that the visibility condition is satisfied. This problem can be understood as a trajectory tracking problem for the UAV. In this section, we first describe a control law which ensures that the UAV exactly tracks the UGV in case that the coverage task is ignored. Then, in the next section, a combined control law is presented for simultaneous tracking and coverage.

If the UGV is not in motion, the trajectory tracking task is nothing but a regulation of the UAV to a constant point in space. However, if the UGV is in motion, the trajectory is time varying and the solution is more sophisticated. Note that the exact tracking problem is solved if the position error $\|\boldsymbol{p}_\Delta\| = \|\boldsymbol{p}_a - \boldsymbol{p}_g\| = 0$. Considering the dynamics of the position error, it follows that

$$\ddot{\boldsymbol{p}}_\Delta = \ddot{\boldsymbol{p}}_a - \ddot{\boldsymbol{p}}_g = \boldsymbol{u}_a - \boldsymbol{u}_g. \tag{13}$$

Therefore, the tracking problem is solved if the error dynamics (13) is stable, since then $\lim_{t\to\infty} \boldsymbol{p}_\Delta(t) = \boldsymbol{0}$. While

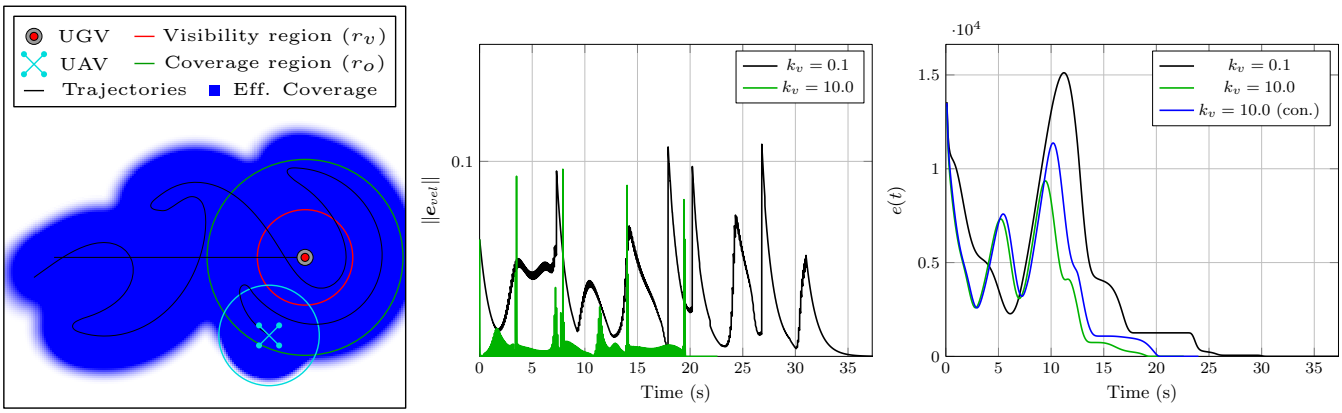

(a) Trajectories and covered area (b) Norm of velocity error (10) for different k_v (c) Coverage error (4) for different k_v

Fig. 1: Example trajectories and error values for different control gains

$\boldsymbol{u}_g$ is determined for the motion of the UGV, the goal is to design $\boldsymbol{u}_a$ for tracking. A straightforward way is to choose $\boldsymbol{u}_a = \boldsymbol{u}_g + \boldsymbol{u}_{a,tr}$, where $\boldsymbol{u}_{a,tr}$ is designed such that $\ddot{\boldsymbol{p}}_\Delta = \boldsymbol{u}_{a,tr}$ is stable. For example, this can be achieved by a state feedback controller

$$\boldsymbol{u}_{a,tr} = -k_0 \boldsymbol{p}_\Delta - k_1 \dot{\boldsymbol{p}}_\Delta, \tag{14}$$

where k_0 and k_1 are chosen such that $\ddot{\boldsymbol{p}}_\Delta + k_1 \dot{\boldsymbol{p}}_\Delta + k_0 \boldsymbol{p}_\Delta = \boldsymbol{0}$ is stable. However, the controller (14) is not only a function of the relative positions $\boldsymbol{p}_\Delta$, but also of the relative velocities $\dot{\boldsymbol{p}}_\Delta$. This implies that the UAV needs information about the velocity of the UGV which is undesirable. To overcome this problem, we use a dynamic control law[1]

$$\dot{\boldsymbol{x}}_c = \boldsymbol{A}_c \boldsymbol{x}_c + \boldsymbol{B}_c \boldsymbol{p}_\Delta \tag{15a}$$

$$\boldsymbol{u}_{a,tr} = \boldsymbol{C}_c \boldsymbol{x}_c + \boldsymbol{D}_c \boldsymbol{p}_\Delta \tag{15b}$$

which needs only the relative position information $\boldsymbol{p}_\Delta$ to stabilize the tracking error dynamics.

Remark 1: Relative localization or the information $\boldsymbol{p}_\Delta$ is available for the UAV, as long as the visibility condition (5) holds. Once the UAV leaves the visibility radius, the tracking controller (15) is useless. Thus, it is necessary to guarantee that the UAV never leaves the visibility radius.

For the above solution, we have assumed that $\boldsymbol{u}_a = \boldsymbol{u}_g + \boldsymbol{u}_{a,tr}$, meaning that the control input of the UGV is available for the UAV. In general, this is not the case unless this information will be communicated. However, we are interested in solutions which rely solely on the relative position error $\boldsymbol{p}_\Delta$.

For this purpose, it should be noted that the input and velocity of the UGV are bounded by their maximum values $u_{g,max}$ and $v_{g,max}$. Hence, if the UGV is in saturation, it moves with a constant maximum velocity towards its target point. In this case, the UGV can be described by an autonomous vehicle with dynamics $\ddot{\boldsymbol{p}}_g = \boldsymbol{0}$ which implies that $\ddot{\boldsymbol{p}}_\Delta = \boldsymbol{u}_a$ and the information $\boldsymbol{u}_g$ is not needed. Only if the UGV is near its target point, where the system is not in saturation and the velocity is not constant, the information $\boldsymbol{u}_g$ is needed for an exact tracking. However, note that the UAV is more flexible and faster than the UGV such that the tracking error close to a target point is negligible. Moreover, it should be considered that the primary goal is to keep the UAV in a region around the UGV (cf. (5)) which does not need an exact tracking and can be ensured without the information $\boldsymbol{u}_g$ in a simple way. We will discuss this issue in the next section.

Summing up, the motion of the UGV can be described sufficiently accurate by piecewise straight lines with dynamics $\ddot{\boldsymbol{p}}_g = \boldsymbol{0}$, and the dynamics of the tracking error reduce to

$$\ddot{\boldsymbol{p}}_\Delta = \boldsymbol{u}_a. \tag{16}$$

Therefore, the controller $\boldsymbol{u}_a = \boldsymbol{u}_{a,tr}$, where $\boldsymbol{u}_{a,tr}$ is given as in (15), solves the tracking problem.

V. COMPLETE MOTION CONTROL

After considering the individual solutions for the tracking problem and dynamic coverage, we can combine the two components to get a complete motion control law that solves the problem posed in Section II.

A. Combined Coverage and Tracking

While there are different ways to combine the above control laws, we can state the most important aspect of the combined control law in general as follows:

Proposition 2: For a system with dynamics as in (1) and $\boldsymbol{u}_{a,tr}$, $\boldsymbol{u}_{a,cov}$ as in (15) and (11), the control law

$$\boldsymbol{u}_a = \alpha(\|\boldsymbol{p}_\Delta\|)\boldsymbol{u}_{a,tr} + \beta(\|\boldsymbol{p}_\Delta\|)\boldsymbol{u}_{a,cov} \tag{17}$$

guarantees $\|\boldsymbol{p}_a(t) - \boldsymbol{p}_g(t)\| < r_v$ for all $t \geq 0$ given the following conditions:

1) The initial states satisfy $\|\boldsymbol{p}_a(0) - \boldsymbol{p}_g(0)\| < r_v$, $\dot{\boldsymbol{p}}_g(0) = \dot{\boldsymbol{p}}_a(0) = \boldsymbol{0}$.
2) $\alpha, \beta : \mathbb{R}_{\geq 0} \to \mathbb{R}_{\geq 0}$ satisfy $\alpha = 1, \beta = 0$ for all $\|\boldsymbol{p}_a(t) - \boldsymbol{p}_g(t)\| \geq r_s$.

[1]The dynamic controller can be converted to an equivalent transfer function $G_r(s) = k\frac{Z(s)}{N(s)}$ (for each input-output channel). As a result, the parameters are simply determined with standard techniques from control theory, e.g., the root locus method.

3) The threshold value r_s is given by

$$r_s = r_v - \frac{1}{u_{a,max}}(v_{g,max}(v_{a,max} + v_{g,max}) + \frac{1}{2}(v_{a,max}^2 - v_{g,max}^2)). \quad (18)$$

Proof: There is an inner radius $r_s < r_v$ around $\boldsymbol{p}_g$ that determines a distance threshold where only the tracking controller will be active. By considering a worst case scenario for a time t_s when $\|\boldsymbol{p}_\Delta(t_s)\| = r_s$, we can calculate the switching distance r_s such that Proposition 2 holds. The worst case scenario is as follows: The UAV moves at $v_{a,max}$ in an arbitrary direction while the UGV moves at $v_{g,max}$ in the opposite direction and $\|\boldsymbol{p}_\Delta(t_s)\| = r_s$ occurs. Now, $\boldsymbol{u}_a = \boldsymbol{u}_{a,tr}$ and the parameters of the tracking controller can be chosen such that the UAV will accelerate with $u_{a,max}$ towards the UGV. The time interval during which $\|\boldsymbol{p}_\Delta\|$ increases can be split into two parts, deceleration to $\|\dot{\boldsymbol{p}}_a\| = 0$ and acceleration to $\|\dot{\boldsymbol{p}}_a\| = v_{g,max}$. Summing up the distances traveled (assuming the UGV still moves away from the UAV) provides (18). As soon as $\|\dot{\boldsymbol{p}}_a\| \geq v_{g,max}$ pointing towards the UGV, the distance will not increase any further which completes the proof. ■

The choice of $\alpha(\|\boldsymbol{p}_\Delta\|)$ and $\beta(\|\boldsymbol{p}_\Delta\|)$ can have a significant influence on how the error (4) evolves. Note that a higher weighting should be given to $\boldsymbol{u}_{a,cov}$ when $\|\boldsymbol{p}_\Delta\|$ is small, meaning that the position tracking is less important when the UAV is closer to the UGV. Several examples of how $\beta(\|\boldsymbol{p}_\Delta\|)$ can be chosen are depicted in Fig. 2. They correspond to the following functions:

$$\alpha_1(\|\boldsymbol{p}_\Delta\|) = \begin{cases} \frac{\|\boldsymbol{p}_\Delta\|}{r_s}, & \text{if } \|\boldsymbol{p}_\Delta\| < r_s \\ 1, & \text{if } \|\boldsymbol{p}_\Delta\| \geq r_s \end{cases}$$

$$\alpha_2(\|\boldsymbol{p}_\Delta\|) = \begin{cases} 0, & \text{if } \|\boldsymbol{p}_\Delta\| < r_s \\ 1, & \text{if } \|\boldsymbol{p}_\Delta\| \geq r_s \end{cases}$$

with $\beta_i(\|\boldsymbol{p}_\Delta\|) = 1 - \alpha_i(\|\boldsymbol{p}_\Delta\|)$, $i = 1, 2$. Another option is $\alpha_3(\|\boldsymbol{p}_\Delta\|) = 1$ and

$$\beta_3(\|\boldsymbol{p}_\Delta\|) = \begin{cases} -k_\beta \log(\frac{\|\boldsymbol{p}_\Delta\|}{r_s}), & \text{if } \|\boldsymbol{p}_\Delta\| < r_s \\ 0, & \text{if } \|\boldsymbol{p}_\Delta\| \geq r_s \end{cases} \quad (19)$$

with $k_\beta > 0$.[2]

In Fig. 3, the distance norm $\|\boldsymbol{p}_\Delta\|$ for the three different combinations is plotted, considering the same scenario as in Fig. 1. Obviously, the visibility condition is always satisfied. Note that $\alpha_1(\|\boldsymbol{p}_\Delta\|)$ and $\beta_1(\|\boldsymbol{p}_\Delta\|)$ represent a linear interpolation strategy between $\boldsymbol{u}_{a,tr}$ and $\boldsymbol{u}_{a,cov}$. Although the linear strategy ensures that the UAV stays within the visibility radius r_v, the solution is somewhat conservative since the allowed distance is not fully utilized. From this point of view, a better result is achieved in case of the switching strategy $\alpha_2(\|\boldsymbol{p}_\Delta\|)$, $\beta_2(\|\boldsymbol{p}_\Delta\|)$. However, the controller causes a sliding mode behavior on the threshold r_s which might be undesirable. The choice $\alpha_3(\|\boldsymbol{p}_\Delta\|)$ and $\beta_3(\|\boldsymbol{p}_\Delta\|)$ describes a

[2]To avoid numerical issues, $\beta_3(\|\boldsymbol{p}_\Delta\|)$ can be limited to a maximum value.

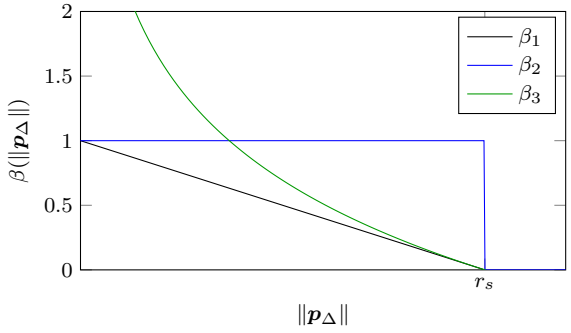

Fig. 2: Different weighting functions

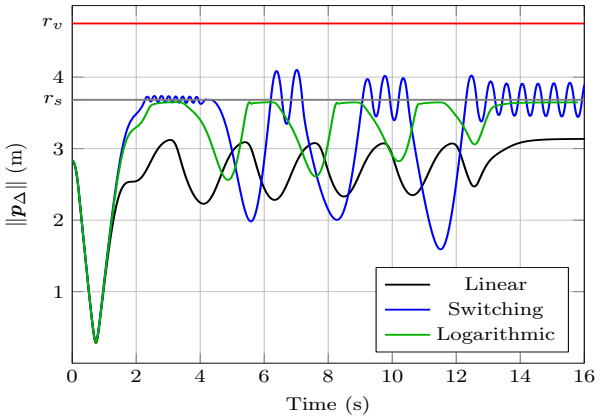

Fig. 3: Distance for different weighting functions

logarithmic interpolation, which provides a tradeoff between the linear interpolation and the switching function. From Fig. 3, it can be seen that the UAV moves closer to the visibility boundary compared to the linear interpolation case, but there is no sliding mode as in the switching strategy.

Remark 2: Under consideration of Proposition 2, other functions for $\alpha(\|\boldsymbol{p}_\Delta\|)$ and $\beta(\|\boldsymbol{p}_\Delta\|)$ are possible. In our simulations, the best results have been achieved with the logarithmic strategy.

B. Virtual Point Tracking

As an alternative to the combined control strategy presented above, we can also omit the coverage part and simply move the UAV along a specified path around the UGV. For instance, the control law can be modified such that the UAV circles with a certain radius around the UGV while tracking its position.

For this purpose, let us define a virtual point $\boldsymbol{p}_v(t)$ such that

$$\mathcal{Q} \ni \boldsymbol{p}_d(t) = \boldsymbol{p}_g(t) + \boldsymbol{p}_v(t). \quad (20)$$

With the help of the virtual point $\boldsymbol{p}_v(t)$, a desired location for the UAV relative to the position of the UGV can be described, where $\|\boldsymbol{p}_v(t)\| < r_v$ must hold to satisfy the visibility constraint (5). The variable $\boldsymbol{p}_d(t)$ can also be interpreted as a trajectory that should be tracked by the UAV, meaning that $\|\boldsymbol{p}_a(t) - \boldsymbol{p}_d(t)\| \to 0$. Thus, as in Section IV, we define the tracking error $\boldsymbol{p}_{\Delta,d} = \boldsymbol{p}_a - \boldsymbol{p}_d$ such that the error dynamics

are determined by

$$\ddot{\boldsymbol{p}}_{\Delta,d} = \boldsymbol{u}_a - \ddot{\boldsymbol{p}}_d. \tag{21}$$

Since we can assume that the dynamics of the UGV are sufficiently accurate described by $\ddot{\boldsymbol{p}}_g = \boldsymbol{0}$, it follows that $\ddot{\boldsymbol{p}}_d = \ddot{\boldsymbol{p}}_v$. Therefore, (21) results in

$$\ddot{\boldsymbol{p}}_{\Delta,d} = \boldsymbol{u}_a - \ddot{\boldsymbol{p}}_v, \tag{22}$$

and defining $\boldsymbol{u}_a = \ddot{\boldsymbol{p}}_v + \boldsymbol{u}_{a,tr}$, we get eventually

$$\ddot{\boldsymbol{p}}_{\Delta,d} = \boldsymbol{u}_{a,tr}. \tag{23}$$

Obviously, the tracking error (23) is described by simple double integrator dynamics which, as before, can be stabilized using the controller (15) where it is just necessary to replace $\ddot{\boldsymbol{p}}_\Delta$ by $\ddot{\boldsymbol{p}}_{\Delta,d}$. Thus, provided that the dynamics of the virtual point $\boldsymbol{p}_v$ is twice differentiable with respect to time, a trajectory tracking controller is given by

$$\boldsymbol{u}_a = \ddot{\boldsymbol{p}}_v + \boldsymbol{u}_{a,tr}. \tag{24}$$

As an example, assume that the UAV moves in a circle around the UGV, then the virtual point $\boldsymbol{p}_v(t)$ can be specified as

$$\boldsymbol{p}_v(t) = \begin{pmatrix} r_{p_v}\cos(\omega_{p_v}t) \\ r_{p_v}\sin(\omega_{p_v}t) \end{pmatrix}, \tag{25}$$

where r_{p_v} and ω_{p_v} are the radius and the frequency of the circular motion respectively.

Remark 3: In case of a constrained system, the parameters of the virtual point motion should be chosen such that the trajectory can be followed by the vehicle without significant tracking error.

VI. SIMULATION RESULTS

In the following, the combined control law and the virtual point tracking method are both illustrated by examples. We implemented the dynamics and controllers in C++ and used the following vehicle parameters: $v_{a,max} = 0.6\frac{\text{m}}{\text{s}}$, $u_{a,max} = 0.3\frac{\text{m}}{\text{s}^2}$, $v_{g,max} = 0.2\frac{\text{m}}{\text{s}}$ and $u_{g,max} = 0.1\frac{\text{m}}{\text{s}^2}$. The sensor characteristics of the UAV are given by $M_a = 1.0$, $r = 5$m, $r_v = 4.75$m and a desired coverage of $C^* = 2.0$. With these values the threshold for the weighting controller is $r_s \approx 3.683$m. We chose a relatively low velocity and acceleration for the UAV to satisfy the assumption of double integrator dynamics.

The controller parameters for $\boldsymbol{u}_{a,tr}$ in (15) are chosen as $\boldsymbol{A}_c = -3$, $\boldsymbol{B}_c = -3$, $\boldsymbol{C}_c = -\frac{8}{3}$, and $\boldsymbol{D}_c = -3$ such that all closed-loop poles are at -1 in an unconstrained system. According to Remark 2, we will use the logarithmic weighting function (19) for the final experiments with $k_\beta = 20$. Finally, a circular motion is specified by the virtual point as in (25) with $r_{p_v} = r_s$ and $\omega_{p_v} = 1\frac{\text{rad}}{\text{s}}$.

Two different experiments are displayed in Fig. 4 and Fig. 5 respectively. The environment is a $40\text{m}\times40\text{m}$ square region in both cases. In the first scenario, the UGV travels through completely uncovered space for all t. Therefore, the error (Fig. 4(c)) is relatively high, but can be kept lower by the dynamic coverage combined with tracking most of the time compared to the circular motion. This difference is even more significant if the UGV travels through regions that are partly covered as in the second scenario. Especially in the beginning, when the UGV moves close to already covered areas (between $t = 0$ and $t = 40$s), the error $e(t)$ is much lower and more consistent when using the coverage strategy (Fig. 5(c)). This result is not unexpected, because the dynamic coverage approach takes the already covered area and density function into account, but it is also the more complex control strategy.

VII. CONCLUSIONS

We have presented some early results on the topic of motion control for a UAV that has to maintain visibility to a UGV, knowing only the UGV's position. Gathering as much information as possible by covering the area was realized with a dynamic coverage strategy and a naive circular motion approach. Both strategies worked well in our experiments, visibility is guaranteed at all times, and have their own advantages. Future work, we are interested in, is the integration and evaluation with a higher level task and realization with hardware. Other interesting points would be control of flight altitude to change the visible area for the UAV, extensions to more than two agents and taking air obstacles into account. More sophisticated motion planning strategies and other uncertainty models for the UAV sensor would also be promising aspects to look into.

REFERENCES

[1] R. Olfati-Saber, "Flocking for multi-agent dynamic systems: Algorithms and theory," *IEEE Transactions on Automatic Control*, vol. 51, no. 3, pp. 401–420, 2006.

[2] H. G. Tanner, A. Jadbabaie, and G. J. Pappas, "Flocking in fixed and switching networks," *IEEE Transactions on Automatic Control*, vol. 52, no. 5, pp. 863–868, 2007.

[3] J. A. Fax and R. M. Murray, "Information flow and cooperative control of vehicle formations," *IEEE Transactions on Automatic Control*, vol. 49, no. 9, pp. 1465–1476, 2004.

[4] P. Ögren and N. E. Leonard, "Obstacle avoidance in formation," in *Proc. Int. Conf. Robotics and Automation*, 2003, pp. 2492–2497.

[5] H. Tanner and D. Christodoulakis, "Cooperation between aerial and ground vehicle groups for reconnaissance missions," in *IEEE Conference on Decision and Control*, 2006, pp. 5918–5923.

[6] N. Michael, S. Shen, K. Mohta, Y. Mulgaonkar, V. Kumar, K. Nagatani, Y. Okada, S. Kiribayashi, K. Otake, K. Yoshida *et al.*, "Collaborative mapping of an earthquake-damaged building via ground and aerial robots," *Journal of Field Robotics*, vol. 29, no. 5, pp. 832–841, 2012.

[7] L. Chaimowicz, B. Grocholsky, J. F. Keller, V. Kumar, and C. J. Taylor, "Experiments in multirobot air-ground coordination," in *IEEE International Conference on Robotics and Automation*, vol. 4, 2004, pp. 4053–4058.

[8] M. Garzón, J. Valente, D. Zapata, and A. Barrientos, "An aerial-ground robotic system for navigation and obstacle mapping in large outdoor areas," *Sensors*, vol. 13, no. 1, pp. 1247–1267, 2013.

[9] A. Dewan, A. Mahendran, N. Soni, and K. M. Krishna, "Heterogeneous UGV-MAV exploration using integer programming," in *IEEE/RSJ International Conference on Intelligent Robots and Systems (IROS)*, 2013, pp. 5742–5749.

[10] B. Grocholsky, J. Keller, V. Kumar, and G. Pappas, "Cooperative air and ground surveillance," *IEEE Robotics & Automation Magazine*, vol. 13, no. 3, pp. 16–25, 2006.

[11] M. Langerwisch, T. Wittmann, S. Thamke, T. Remmersmann, A. Tiderko, and B. Wagner, "Heterogeneous teams of unmanned ground and aerial robots for reconnaissance and surveillance-a field experiment," in *IEEE International Symposium on Safety, Security, and Rescue Robotics (SSRR)*, 2013, pp. 1–6.

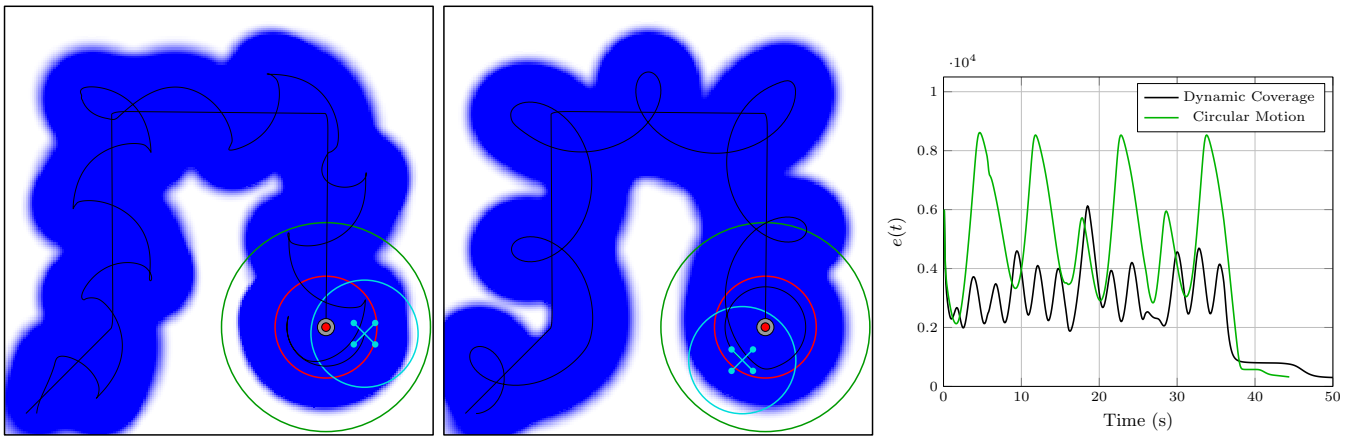

(a) Dynamic coverage trajectories (b) Circular motion trajectories (c) Comparison of $e(t)$

Fig. 4: Simulation results for scenario 1

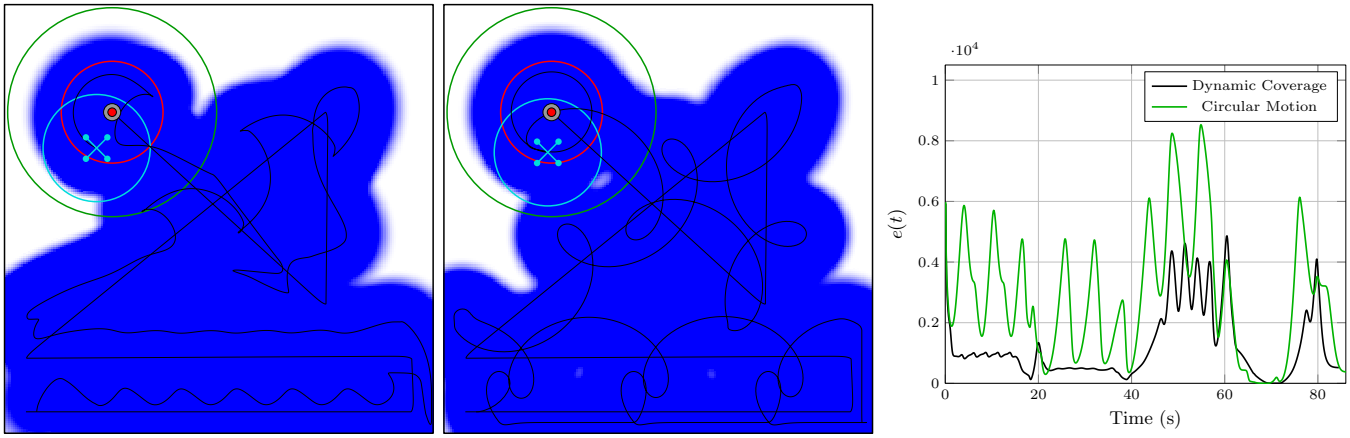

(a) Dynamic coverage trajectories (b) Circular motion trajectories (c) Comparison of $e(t)$

Fig. 5: Simulation results for scenario 2

[12] C. Forster, M. Pizzoli, and D. Scaramuzza, "Air-ground localization and map augmentation using monocular dense reconstruction," in *IEEE/RSJ International Conference on Intelligent Robots and Systems*, 2013, pp. 3971–3978.

[13] L. Cantelli, M. Mangiameli, C. Melita, and G. Muscato, "UAV/UGV cooperation for surveying operations in humanitarian demining," in *IEEE International Symposium on Safety, Security, and Rescue Robotics (SSRR)*, 2013, pp. 1–6.

[14] G. Heppner, A. Roennau, and R. Dillman, "Enhancing sensor capabilities of walking robots through cooperative exploration with aerial robots," *Journal of Automation, Mobile Robotics & Intelligent Systems*, vol. 7, no. 2, pp. 5–11, 2013.

[15] W. Li, T. Zhang, and K. Kuhnlenz, "A vision-guided autonomous quadrotor in an air-ground multi-robot system," in *IEEE International Conference on Robotics and Automation*, 2011, pp. 2980–2985.

[16] M. Saska, V. Vonásek, T. Krajník, and L. Přeučil, "Coordination and navigation of heterogeneous MAV–UGV formations localized by a hawk-eye-like approach under a model predictive control scheme," *The Int. Journal of Robotics Research*, vol. 33, pp. 1393–1412, 2014.

[17] E. Mueggler, M. Faessler, F. Fontana, and D. Scaramuzza, "Aerial-guided navigation of a ground robot among movable obstacles," in *IEEE International Symposium on Safety, Security, and Rescue Robotics (SSRR)*, 2014, pp. 1–8.

[18] I. I. Hussein and D. M. Stipanović, "Effective coverage control using dynamic sensor networks," in *45th IEEE Conference on Decision and Control*, 2006, pp. 2747–2752.

[19] ——, "Effective coverage control for mobile sensor networks with guaranteed collision avoidance," *IEEE Transactions on Control Systems Technology*, vol. 15, no. 4, pp. 642–657, 2007.

[20] L. C. Pimenta, M. Schwager, Q. Lindsey, V. Kumar, D. Rus, R. C. Mesquita, and G. A. Pereira, "Simultaneous coverage and tracking (SCAT) of moving targets with robot networks," in *Algorithmic Foundation of Robotics VIII*. Springer, 2010, pp. 85–99.